Approximating Kinematics for Tracked Mobile Robots

Article *in* The International Journal of Robotics Research · October 2005

DOI: 10.1177/0278364905058239 · Source: DBLP

5 authors, including:

Jorge L. Martínez
University of Malaga
76 PUBLICATIONS **1,118** CITATIONS
SEE PROFILE

Anthony Mandow
University of Malaga
72 PUBLICATIONS **1,050** CITATIONS
SEE PROFILE

J. Morales
University of Malaga
44 PUBLICATIONS **717** CITATIONS
SEE PROFILE

Salvador Pedraza
University of Oulu
5 PUBLICATIONS **158** CITATIONS
SEE PROFILE

J. L. Martínez
A. Mandow
J. Morales
S. Pedraza
A. García-Cerezo

Dept. Ingeniería de Sistemas y Automática
Universidad de Málaga
Plaza El Ejido s/n, 29013-Málaga, Spain
jlmartinez@uma.es

Approximating Kinematics for Tracked Mobile Robots

Abstract

In this paper we propose a kinematic approach for tracked mobile robots in order to improve motion control and pose estimation. Complex dynamics due to slippage and track–soil interactions make it difficult to predict the exact motion of the vehicle on the basis of track velocities. Nevertheless, real-time computations for autonomous navigation require an effective kinematics approximation without introducing dynamics in the loop. The proposed solution is based on the fact that the instantaneous centers of rotation (ICRs) of treads on the motion plane with respect to the vehicle are dynamics-dependent, but they lie within a bounded area. Thus, optimizing constant ICR positions for a particular terrain results in an approximate kinematic model for tracked mobile robots. Two different approaches are presented for off-line estimation of kinematic parameters: (i) simulation of the stationary response of the dynamic model for the whole velocity range of the vehicle; (ii) introduction of an experimental setup so that a genetic algorithm can produce the model from actual sensor readings. These methods have been evaluated for on-line odometric computations and low-level motion control with the Auriga-α mobile robot on a hard-surface flat soil at moderate speeds.

KEY WORDS—tracked vehicles, kinematic control, mobile robotics, parameter identification, dynamics simulation

1. Introduction

Locomotion based on tracks offers a large contact area with the ground, which provides better traction than wheels for vehicles on natural terrains (Bekker 1956). Thus, tracked mobile robots can be useful in applications such as agriculture, search and rescue, military, forestry, mining and planetary exploration.

The International Journal of Robotics Research
Vol. 24, No. 10, October 2005, pp. 867-878,
DOI: 10.1177/0278364905058239

Steering of tracked vehicles has certain unique features that make it quite different from the case of wheeled vehicles. Consequently, it requires special treatment. Several track configurations for steering have been proposed: articulated steering, curved track steering, and skid steering (Wong 2001). The latter is the most widely used, since it is simpler from the mechanical standpoint and it achieves a faster response (Kar 1987).

The skid steering principle is based on controlling the relative velocities of both tracks, much in the same way as differential drive wheeled vehicles. However, control of tracked locomotion poses a more complex problem because variation of the relative velocity of the two tracks results in slippage as well as soil shearing and compacting in order to achieve steering (see Figure 1).

Thus, kinematics is not straightforward, since it is not possible to predict the exact motion of the vehicle only from its control inputs. This means that motion control methods suitable for differential wheeled robots (Ollero et al. 1997) cannot be directly used for tracked vehicles (or, at least, not in a reliable way).

In spite of these difficulties, an effective kinematic model would allow prediction of the approximate motion of the vehicle in the short term, which is necessary to perform onboard real-time computations for autonomous navigation.

The shortcomings of wheels on certain types of terrain was one of the lessons learned from our experience in agricultural robotics (Mandow et al. 1996), which led to the design and construction of the Auriga-α tracked robot (Pedraza et al. 2000). In our earliest control efforts with Auriga-α, a simple differential drive model, which considered tracks as wheels, was assumed. As expected, this model achieved less than adequate results because it did not consider slippage. Since then, alternative heuristic, analytical and experimental solutions have been worked out to enhance control and odometry. The work presented in this paper summarizes these efforts.

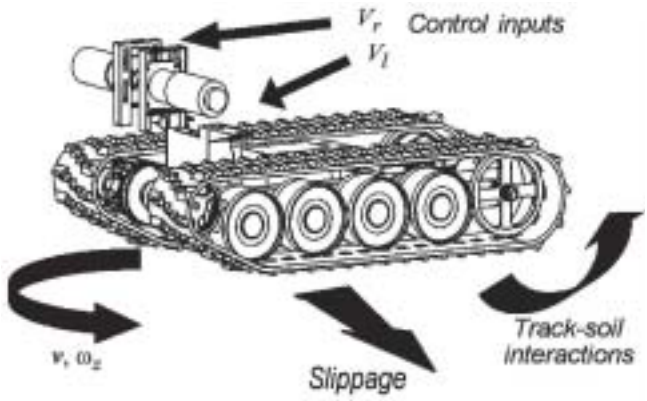

Fig. 1. Skid steering principle.

The proposed approach is to model kinematics for tracked vehicles by obtaining a geometric analogy with a wheeled differential drive model. This model can be tuned by means of off-line parameter identification, which can be derived either from the simulation of a dynamic model or from actual experimental data. Certain simplifying constraints have been considered: planar uniform hard terrain type, and mobile robot operation at moderate speeds.

Following this introduction, in Section 2 we review antecedents in control for tracked vehicles. In Section 3 we address kinematic modeling based on the instantaneous centers of rotation of the two tracks on the plane. Section 4 offers solutions for identifying approximate kinematic parameters from simulated and experimental data. In Section 5 we present details on the implementation of kinematic models for the Auriga-α mobile robot. Validation experiments for these models are discussed in Section 6. Section 7 is devoted to conclusions and ideas for future work. Finally, acknowledgments and references complete the paper.

2. Related Work

Abundant theoretical research on terramechanics has been devoted to the study of mechanics, modeling techniques and track–soil interaction of tracked vehicles (Wong 2001). This theoretical background has allowed simulation of this type of vehicle, which has become a powerful tool for designing and evaluating different configurations (Ferretti and Girelli 1999). In contrast, little work has been reported on the particular problem of motion control for tracked autonomous mobile robots.

Relevant works devoted to tracked motion control are the following.

- Wang, Wang, and Chen (1990) consider the vehicle as a non-linear two-input two-output system, whose behavior is modeled by two linear black boxes with uncertain parameters. Two robust controllers are obtained to control translational and angular velocities.

- Shiller, Serate, and Hua (1993) address the problem of determining nominal track forces to follow a planned path at specified speeds. Lateral friction dynamics are considered in the optimization of vehicle's orientation. Tests are reported for circular paths on flat and inclined planes.

- The work of Fan, Koren, and Wehe (1995) is devoted to straight line motion control for an actual tracked platform. The authors discuss cross-coupling control in order to cope with the differences in response of both tracks. Besides, an adaptive parameter is considered for errors due to mechanical asymmetries during wall following.

- Fan et al. (1995) are concerned with pose estimation for tracked mobile robots. Instead of odometry from the vehicle itself, the authors propose adding a small passive two wheeled trailer. Encoders are located in each wheel and in the trailer joint.

- Le, Rye, and Durrant-Whyte (1997) address identification of track slippage without previous knowledge of soil characteristics. A kinematic model of the vehicle relates the slip parameters to the track velocities. Estimation is performed from actual inertial readings with an extended Kalman filter. The authors propose identification of soil properties to adjust motion control.

- Ahmadi, Polotski, and Hurteau (2000) adapt a path-tracking algorithm for wheeled robots by feedback linearization of the complex force–slip relationship. A simplified model of dynamic friction forces is used for feedforward compensation. The controller is tested to follow arbitrary trajectories.

All these authors agree in the fact that motion control for tracked vehicles is a very complicated problem, where a general solution has not yet been reached. Furthermore, most published works are based on simulated results and use complex vehicle dynamics in some way.

3. Kinematics for Tracked Vehicles

Dynamic models of tracked vehicles have proved to be helpful for control design and reliable simulation, but they may be too costly for real-time robot navigation. Alternatively, in this section we discuss geometric relationships that can be used instead.

The local frame of the vehicle is assumed to have its origin on the center of the area defined by contact surface of both tracks on the plane, and its Y-axis is aligned with the forward

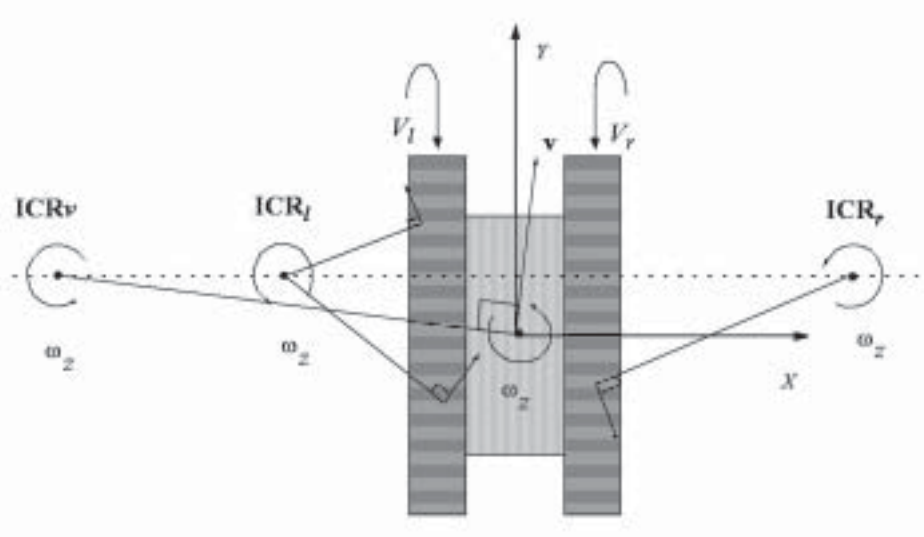

Fig. 2. ICRs on the plane. The entire vehicle as a rigid body follows a circular course about $\mathbf{ICR}_v$.

motion direction. Much in the same way as with wheeled differential drive, a tracked vehicle is governed by two control inputs: the linear velocity of its left and right tracks with respect to the robot frame (V_l, V_r). Then, direct kinematics on the plane can be stated as follows:

$$(v_x, v_y, \omega_z) = f_d(V_l, V_r) \tag{1}$$

where $\mathbf{v} = (v_x, v_y)$ is the vehicle's translational velocity with respect to its local frame, and ω_z is its angular velocity. Conversely, finding control actions that result in a desired motion can be expressed as the inverse kinematics problem:

$$(V_l, V_r) = f_i(v_x, v_y, \omega_z). \tag{2}$$

If the vehicle is considered as a rigid body with planar motion, then its instantaneous center of rotation ($\mathbf{ICR}_v$) is defined as the point in the horizontal plane where the motion of the vehicle can be represented by a rotation and no translation occurs. This point can be expressed in local coordinates as $\mathbf{ICR}_v = (x_{ICRv}, y_{ICRv})$, as shown in Figure 2.

In the planar motion of a tracked vehicle, it would be interesting to take into account not only the behavior of the entire body, but also the motion of both its tracks on their contact surface with the ground. A track can be modeled as another rigid body with an extra degree of freedom, which is its rolling speed. Thus, the motion of a point in the tread surface is the composition of the motion of the vehicle and that of track rolling. Because of this, the ICR of a track on the plane is different from the ICR of the entire vehicle. Then, the ICRs for the left and right tracks can be defined in the local frame as $\mathbf{ICR}_l = (x_{ICRl}, y_{ICRl})$ and $\mathbf{ICR}_r = (x_{ICRr}, y_{ICRr})$, respectively (see Figure 2). Note that this definition refers to the ICR of track treads on the ground plane, not to their roll axis.

Interestingly, because of Kennedy's ICR theorem (Shigley and Uicker 1980), it is known that $\mathbf{ICR}_l$ and $\mathbf{ICR}_r$ lie on a line parallel to the local X-axis, which also contains $\mathbf{ICR}_v$. Furthermore, the Z component of the angular velocity of the two tracks on the plane is the same as that of the vehicle, since they cannot rotate around the vehicle's Z-axis.

Local coordinates for the vehicle and track ICRs can be obtained geometrically as a function of the vehicle's angular and translational velocities as

$$x_{ICRv} = \frac{-v_y}{\omega_z} \tag{3}$$

$$x_{ICRl} = \frac{V_l - v_y}{\omega_z} \tag{4}$$

$$x_{ICRr} = \frac{V_r - v_y}{\omega_z} \tag{5}$$

$$y_{ICRv} = y_{ICRl} = y_{ICRr} = \frac{v_x}{\omega_z}. \tag{6}$$

The values of x_{ICRv} range within $\pm\infty$ depending on the vehicle's curvature; the infinite values are reached when $\omega_z = 0$ in eq. (3). However, it must be noted that the same does not apply for tread ICR coordinates x_{ICRl}, x_{ICRr} and y_{ICRv}, which are bounded: in the proximity of straight line motion, numerators and denominators in eqs. (4)–(6) are infinitesimals of the same order, which result in finite values for x_{ICRl}, x_{ICRr} and y_{ICRv}, respectively.

If the inverse functions are computed from eqs. (3)–(6), instantaneous translational and rotational speeds with respect

to the local frame can be obtained as

$$v_x = \frac{V_r - V_l}{x_{ICRr} - x_{ICRl}} y_{ICRv} \tag{7}$$

$$v_y = \frac{V_r + V_l}{2} - \frac{V_r - V_l}{x_{ICRr} - x_{ICRl}} \left(\frac{x_{ICRr} + x_{ICRl}}{2} \right) \tag{8}$$

$$\omega_z = \frac{V_r - V_l}{x_{ICRr} - x_{ICRl}}. \tag{9}$$

These equations represent the vehicle's direct kinematics as stated by eq. (1) assuming that the ICRs of the left and right treads could be properly estimated. Note in eq. (7) that if the ICRs lie precisely on the local X-axis (i.e., $y_{ICRv} = 0$), then the vehicle's velocity **v** has no transversal component (i.e., $v_x = 0$).

On the other hand, inverse kinematic relations can be expressed by

$$V_l = v_y + x_{ICRl}\,\omega_z \tag{10}$$

$$V_r = v_y + x_{ICRr}\,\omega_z, \tag{11}$$

which includes a non-holonomic restriction, since v_x references cannot be directly imposed. Besides, according to these equations, the same control input values are computed regardless of y_{ICRv} in the model.

It must be noted that the above expressions also represent direct and inverse kinematics for the particular case of ideal wheeled differential drive vehicles, as illustrated by Figure 3. Therefore, for instantaneous motion, kinematic equivalences can be considered between tracked and ideal wheel vehicles.

The difference between both traction schemes is that whereas ICRs for ideal wheels without lateral sliding are constant and coincident with the ground contact points, track ICRs are dynamics-dependent and always lie outside the track centerlines because of slippage. Thus, less track slippage results in track ICRs that are closer to the vehicle.

Moreover, the center of mass of a vehicle significantly affects track ICRs. If it is closer to one side, then that side's track will slip less on account of pressure and its ICR will be closer to the vehicle. Conversely, the opposite track ICR will be farther. Furthermore, less slippage occurs in both tracks if the center of mass is closer to the front or rear end of the vehicle, since pressure distribution concentrates onto a portion of the track contact surface. This results in closer track ICRs. These effects can be quantified by stating appropriate indexes.

A steering efficiency index χ of the vehicle can be defined as the inverse of the normalized distance between the track ICRs

$$\chi = \frac{L}{x_{ICRr} - x_{ICRl}};\ (0 < \chi \leqslant 1), \tag{12}$$

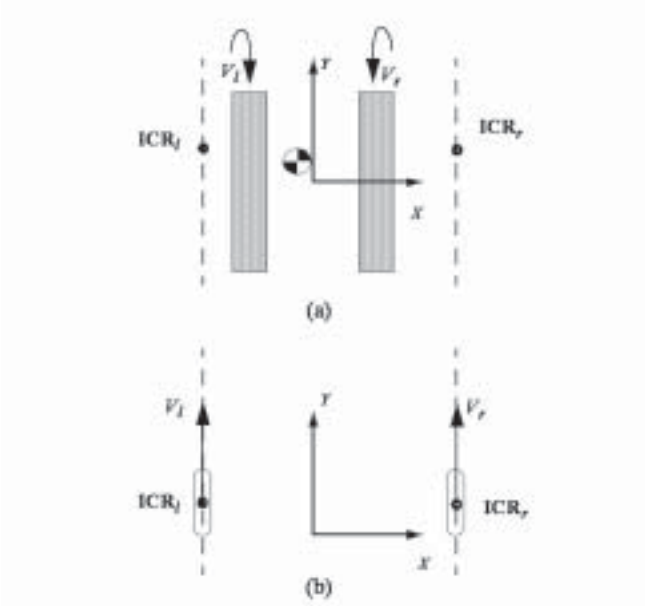

Fig. 3. Geometric equivalence of instantaneous motion for (a) tracked and (b) wheeled differential drive kinematics.

where L is the distance between track centerlines. Index χ is equal to 1 when no slippage occurs (i.e., ideal differential drive).

Similarly, a normalized eccentricity index can be defined as follows:

$$e = \frac{x_{ICRr} + x_{ICRl}}{x_{ICRr} - x_{ICRl}}. \tag{13}$$

Index e is zero when track ICRs are symmetrical with respect to the local Y-axis.

The major consequence of the discussion above is that the effect of vehicle dynamics is introduced in the kinematic model just by two points in local coordinates: **ICR**$_l$ and **ICR**$_r$. These points are bounded variables for tracked vehicles and coincide with wheel contact points for ideal differential drive.

4. Identification of Tracked Kinematic Parameters

In this section we describe how the analogies presented in Section 3 have been considered to approximate a dynamics-free tracked kinematic model. This implies identifying optimized constant values for track ICRs given a set of working conditions, which can be considered as finding contact points for an equivalent wheeled vehicle. Optimization is required, since actual track ICR positions vary during navigation on account of dynamics.

Thus, the identification problem consists on finding three parameters:

- the local Y coordinate of track ICRs ($y_{ICRl} = y_{ICRr} = y_{ICRv}$).
- the local X coordinates of both track ICRs (x_{ICRr} and x_{ICRl}).

Two different off-line approaches are presented in order to fit approximate values for these parameters. In the first place, these can be optimized from the simulation of the stationary response of the dynamic model of the vehicle for its whole velocity range. Alternatively, two experimental methods are presented to obtain the model from actual sensor readings: one uses only internal sensor data to compute a symmetric model; the other achieves a more realistic model by feeding a genetic algorithm with raw trajectory data and reliable localization estimations based on external sensors.

4.1. Derivation of Track ICRs from the Simulation of the Dynamic Model

An analytical study of the stationary response based on a computer simulation of vehicle and terrain type dynamics can be used to calculate approximate track ICR positions (Pedraza 2000). Since motor drives with large reduction act as low pass filters, the stationary response of the dynamic system provides a good approximation of its kinematic behavior.

Basically, the dynamic model consists of force and moment equations dependent on soil mechanics and vehicle dynamics. The general dynamic equations that describe the robot's motion are the following

$$m\,\boldsymbol{v}'_{\mathbf{cog}} = \sum \mathbf{F} \tag{14}$$

$$\boldsymbol{\omega}'\,[\mathbf{I}] + \sum_{\Omega} \boldsymbol{\tau}_{\mathbf{i}} = \sum (\mathbf{r} \times \mathbf{F}), \tag{15}$$

where m is the mass of the whole vehicle, $\mathbf{v}_{cog}$ is the velocity of its center of gravity with respect to the inertial frame, $\mathbf{F}$ are the external forces, $[\mathbf{I}]$ is the inertia matrix with respect to its center of gravity, $\boldsymbol{\omega}$ is the angular velocity vector, $\mathbf{r}$ is the position of the point where forces are applied with respect to the center of gravity, and $\boldsymbol{\tau}_{\mathbf{i}}$ are the torques due to acceleration and gyroscopic effects of the set of internal moving parts of the vehicle (Ω).

The force field that the ground effects onto the tracks can be decomposed into two mutually orthogonal fields. First, the pressure field is perpendicular to the contact plane and opposes to the weight of the vehicle. Secondly, friction forces are parallel to the contact plane and are responsible for the motion. Besides, the effects that the vehicle produces on the ground, such as compaction and erosion, cause motion resistance that must be considered in the model.

It must be noted that in the case of non-hard terrains, resistance forces play a relevant role in the track ICR positions. In this case, the kinematic approach can effectively be applied if different parameter sets for the track ICRs are tabulated depending on the different combinations of the signs of the track velocities and their relative difference (Pedraza 2000). However, at high speed, inertial forces become relevant and severely affect track ICRs, which makes the proposed kinematic approach ineffective.

All dynamic parameters in this model have to be identified from a detailed analysis of the vehicle, its tracks and the soil. Given the dynamic model, the stationary problem can be solved for a number of combinations of track speeds along the whole velocity range of the actuators. Different track ICR positions are obtained from each combination. An approximate optimized constant value for the track ICRs can then be averaged from the whole solution map.

In this way, it is not necessary to use the actual robot for computing the track ICR estimations. Nevertheless, a dynamic model has to be calculated beforehand, which represents only an approximation of the actual vehicle–soil interactions. Moreover, parameters are optimized for a homogeneous wide-range combination of track speeds that is independent of the type of paths to be performed eventually by the actual robot.

4.2. Experimental Identification of Track ICRs

A simple differential drive model for tracked locomotion (supposing symmetric track ICRs, i.e., $e = 0$ and $y_{ICR} = 0$) can be obtained by just taking into account the loss of steering efficiency introduced by slippage. Under this assumption, equivalent ideal wheels would be placed symmetrically on the X-axis some distance away from the track centerlines, i.e., $x_{ICRl} = -x_{ICRr}$ and $x_{ICRr} > \mathrm{L}/2$. Steering efficiency χ can be estimated from a simple experiment with the actual robot and terrain setup (Pedraza et al. 2000).

When equal opposite track speed control inputs V_r and V_l are issued, the vehicle exhibits an approximately pure rotation about its Z-axis. Then, the following equation can be applied

$$\chi = \frac{L\,\phi}{\int V_r \mathrm{d}t - \int V_l \mathrm{d}t}, \tag{16}$$

where ϕ represents the actual rotated angle. The value of x_{ICRr} can then be computed from eq. (12).

This simple method offers a kinematic solution that accounts for track slippage. However, it does not contemplate the effects of the center of mass.

A more complex experimental setup has to be considered so that independent ICR coordinates are estimated for both tracks. In this case, the proposed parameter identification method comprises two steps. The first is to obtain experimental data from external as well as internal sensors. Then, an optimization tool is employed to find the parameter values that best fit the data.

Genetic algorithms (GAs) are proposed as an appropriate search method for this problem. This is a derivative-free stochastic optimization tool, where each point in a solution space is encoded into a bit string (chromosome) and is associated with a fitness value. Starting from an initial random population, points with better fitness values are used to construct a new population of solutions by means of genetic operators. Thus, after several iterations (generations), the overall fitness value is improved.

GAs are useful for finding optimized track ICR parameters (x_{ICRl}, x_{ICRr}, y_{ICRv}) from experimental data because no significant a priori knowledge exists about them, it is straightforward to code them as bit strings, and a way can be devised to assign a fitness value to new solutions (Martínez et al. 2004).

Data collection experiments consist of a limited number of actual paths on a particular soil type, in which the vehicle is subject to diverse rotational and translational speeds and accelerations. Data logged from internal readings (e.g., shaft encoders or inertial sensors) are needed to replay odometric estimations according to alternative kinematic parameters. External sensor readings (e.g., from a laser scanner or DGPS) occur at a lower rate, and are necessary to accurately determine the actual position of the vehicle. Thus, training paths can be broken into a number N of short segments according to the external sensor rate, in such a way that each segment contains several consecutive internal readings as well as accurate relative localization between the final and the starting poses.

Fitness of the alternative solutions evaluated by the GA can be assessed by computing the sum of the squared odometric errors for the N recorded segments

$$J(x_{ICR_l}, x_{ICRr}, y_{ICR_v}) = \sum_{i=1}^{N} \left(\left(\Delta x_i - \Delta \hat{x}_i\right)^2 + \left(\Delta y_i - \Delta \hat{y}_i\right)^2 + \left(\Delta \phi_i - \Delta \hat{\phi}_i\right)^2 \right), \quad (17)$$

where $(\Delta \hat{x}_i, \Delta \hat{y}_i, \Delta \hat{\phi}_i)$ is the estimated pose increment of the vehicle obtained by integrating eqs. (7)–(9) along the ith segment, and $(\Delta x_i, \Delta y_i, \Delta \phi_i)$ denotes the actual localization of the vehicle relative to the origin of each segment.

Thus, at each GA iteration, a number of solutions with minimum overall error are chosen for computing a new population with the crossover and mutation operators. As a result, constant ICR parameters (x_{ICRl}, x_{ICRr}, y_{ICRv}) can be optimized off-line for a specific robotic task, according to typical path motions, particular soil types, and speed ranges.

Moreover, this method can straightforwardly be adapted to incorporate additional search parameters that would result in a more realistic kinematic model. For instance, eqs. (1) and (2) rely on track velocities (V_l, V_r), which are estimated from drive sensor readings following a linear scaling as

$$V_l = K \omega_{ld} \quad (18)$$

$$V_r = K \omega_{rd} \quad (19)$$

where ω_{ld} and ω_{rd} are the angular velocities of the left and right drive shafts according to internal readings. Scale factor K is a constant nominal value calculated for the vehicle according to technical specifications for sensor resolution, gear ratio, sprocket diameter and track belt width.

However, translation of these readings into track velocities can be inaccurate due to issues that are difficult to account for, such as track wear and mechanical misalignments (Fan, Koren, and Wehe 1995). Hence, the actual relation between track speeds and drive shaft velocities would be better expressed by

$$V_l = (K \alpha_l) \omega_{ld} \quad (20)$$

$$V_r = (K \alpha_r) \omega_{rd} \quad (21)$$

where α_l and α_r are correction factors to the known nominal value of K. Parameters α_l and α_r can be experimentally identified to fine-tune the kinematic model by introducing them into the chromosome for the GA search method described above.

The GA search method can readily produce parameters from the real system as long as reliable pose estimations are available. As usual with identification problems, this method captures actual working conditions.

5. Implementation for the Auriga-α Mobile Robot

5.1. Auriga-α Mobile Robot

The methods presented in this paper have been applied to obtain an approximate kinematic model for the Auriga-α mobile robot (see Figure 4). Its dimensions are 1.24(l) × 0.75(w) × 0.84(h) m^3, and it weighs approximately 258 kg. This vehicle is powered by an on-board petrol-fed AC generator, although a power cable socket is also available for indoor tests.

Locomotion is based on two independent DC motors fitted with 1:38 gear reductions and incremental shaft encoders for dead reckoning. Each track contains four rollers as well as sprockets at both ends, of which the foremost one is linked to the output gear shaft. The rubber belts are 0.15 m wide, with a longitudinal contact surface of 0.7 m and L = 0.42 m. The maximum speed of each track is 1 m s^{-1}.

Two control systems can be distinguished in the mobile robot Auriga-α:

- the DSP-based motor control interface, which accepts track speed setpoints from either the manual control joystick or the navigation controller and also provides actual track speeds;
- the navigation system, which includes the low-level controller and the path tracker. An industrial PC based

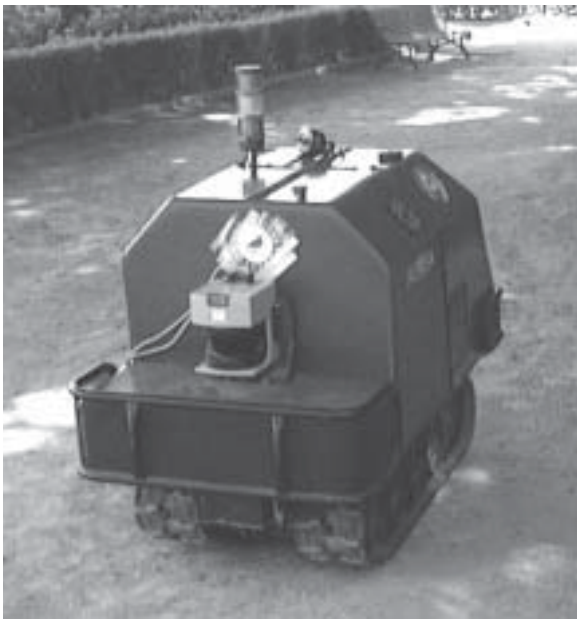

Fig. 4. The Auriga-α mobile robot.

on a Pentium-IV microprocessor at 2.2 GHz governs navigation under a real-time operating system every T_c = 30 ms.

The external sensor employed for self-localization is an onboard conventional time-of-flight range scanner (LMS-200), which scans a plane parallel to the ground at a height of 0.55 m in front of the vehicle. Every T_L = 0.27 s, a new scan is transmitted to the navigation PC through a serial port.

5.2. Dynamic Modeling

A number of considerations have been introduced in order to obtain a dynamic model for the Auriga-α robot on a hard-surface soil, according to eqs. (14) and (15). Thus, gyroscopic torques produced by the rotation of internal elements of the vehicle have been neglected in the model. As for external forces, gravitative attraction and track–soil effects have been considered. Track–soil interaction is modeled by pressure and friction fields. Since compaction and erosion are negligible for hard soils, motion resistance has not been considered. Also, the inertial forces and aerodynamic resistance have been discarded due to the moderate speed assumption.

Regarding pressure distribution, a two-dimensional model for the track contact area has been adopted, as shown in Figure 5. This distribution, which is affected by the position of the center of gravity and by dynamic effects, is linear in the longitudinal axis and transversely constant.

For friction, in the case of hard-surface soils, the resulting force for a point in the track is a function of its slip velocity

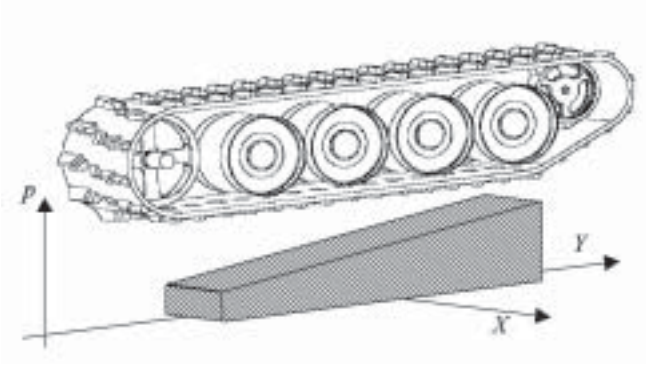

Fig. 5. Linear two-dimensional pressure (p) model.

$\mathbf{v}_s$ as expressed by Coulomb's law

$$\boldsymbol{\tau} = -[\boldsymbol{\mu}]\ p\frac{\boldsymbol{\upsilon}_\mathbf{s}}{|\boldsymbol{\upsilon}_\mathbf{s}|} \tag{22}$$

where p is the pressure under the track, and $[\boldsymbol{\mu}]$ is a coefficient matrix, which, in the general case of anisotropic friction on the XY plane, has the following form:

$$[\boldsymbol{\mu}] = \begin{bmatrix} \mu_x & 0 & 0 \\ 0 & \mu_y & 0 \\ 0 & 0 & 0 \end{bmatrix}. \tag{23}$$

Moreover, if the inertia frame coincides with the vehicle frame, $[\mathbf{I}]$ is a diagonal matrix expressed as

$$[\mathbf{I}] = \begin{bmatrix} I_x & 0 & 0 \\ 0 & I_y & 0 \\ 0 & 0 & I_z \end{bmatrix}. \tag{24}$$

This model has been simulated for computing track ICR positions for the Auriga-α robot. Particularly, the solution of the stationary problem has been obtained for all the left–right combinations of equidistant track speeds in the (–1, +1 m s^{-1}) range, which results in a map of track ICR positions. Figure 6 shows such a map under the simplifying assumption that the center of mass of the vehicle is at the origin of the local frame, which produces a symmetrical distribution of track ICR positions with respect to the Y-axis. The map depicted in Figure 7 takes into account the actual position of the center of mass, which has been estimated as (–0.015 m, 0.04 m). It can be observed that less dispersion occurs in ICR_l points than in ICR_r points, since the left track experiences more pressure and, consequently, less slippage.

By averaging the maps, constant coordinates for track ICRs can be fit to the overall stationary response of the dynamic model. The mean values in the case of the symmetric model (i.e., e = 0) are x_{ICRl} = –0.422 m, x_{ICRr} = 0.422 mm, and y_{ICRv} = 0 m, which correspond to an efficiency index of χ = 0.497. In the case of the asymmetric map shown in Figure 7,

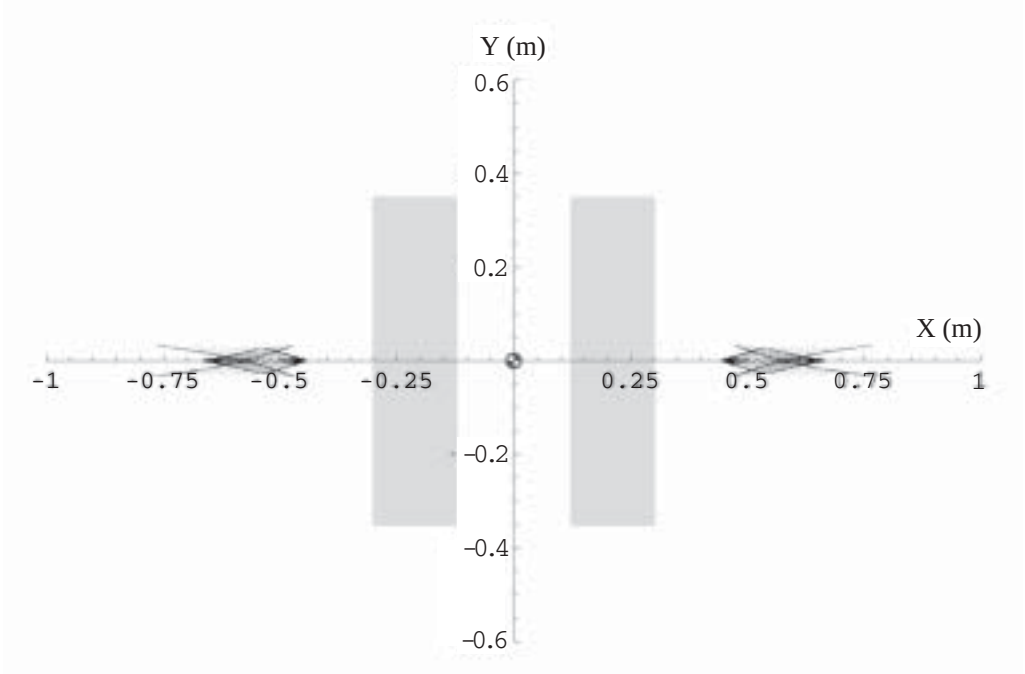

Fig. 6. Dynamic analysis of track ICRs for the Auriga-α mobile robot assuming the center of mass on the frame origin.

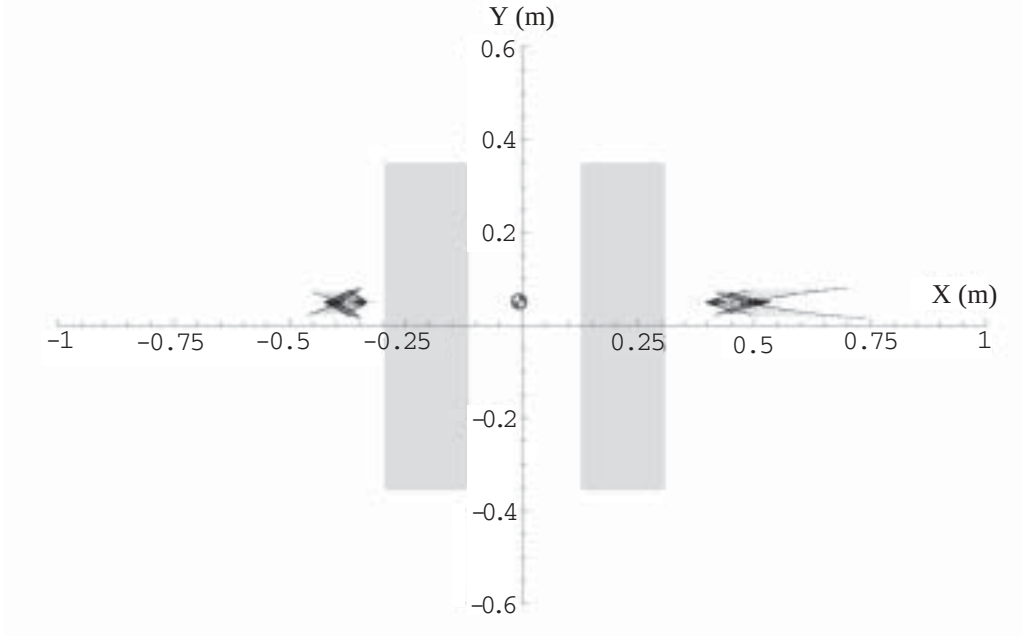

Fig. 7. Dynamic analysis of track ICRs for the Auriga-α mobile robot based on the estimated position of the center of mass.

averaging yields x_{ICRl} = –0.375 m, x_{ICRr} = 0.457 m, and y_{ICRv} = 0.0492 m, with efficiency and eccentricity values of χ = 0.505 and e = 0.108, respectively.

5.3. Experimental Identification

Of the two experimental approaches presented in Section 4.2, the simpler symmetrical model was obtained as the average value given by eq. (16) for several tests (Pedraza et al. 2000). The result was χ = 0.526, which means that the track ICR coordinates are $\mathbf{ICR}_l$ = (–0.399 m, 0) and $\mathbf{ICR}_r$ = (0.399 m, 0). Even though this method does not consider eccentricity, it provides a good approximation to the steering efficiency index obtained in Section 5.2 from the dynamic analysis of the vehicle.

The second experimental approach aims to obtain a more realistic asymmetric model of vehicle kinematics by GA identification. In data gathering experiments, shaft encoder readings were recorded for every control interval (T_c = 0.03 s). Besides, 180° range streams from the onboard laser scanner where periodically recorded at scan intervals (T_L = 0.27 s), so that they could be used in combination with a reliable localization procedure that matches consecutive scans (Martínez 2003).

The training experiments consisted of nine different manually guided paths (about 20 m long each) over a flat hard-surface soil. These resulted in N = 1807 segments of 0.27 s that contain nine sets of successive odometric readings each. The GA method has been applied to search ICR parameters that optimize odometric estimations for the total number of segments, reaching values x_{ICRl} = –0.353 m, x_{ICRr} = 0.425 m, and y_{ICRv} = 0.032 m, with efficiency and eccentricity values of χ = 0.55 and e = 0.092, respectively.

The solutions obtained from the simulated and experimental methods are summarized in Figure 8. From a qualitative standpoint, experimental results are coherent with those obtained in simulation. Thus, the estimated track ICRs are not symmetrical with respect to the Y local axis, and lie on a line at a certain distance ahead of the X-axis. Nevertheless, the experimental model reveals a greater degree of slippage than the dynamic analysis.

6. Experimental Validation

The sets of kinematic parameters computed in the previous section have been used to perform odometric estimations over a number of test paths. These paths are different from those used in the GA experimental procedure, but they were run in the same environment. Two representative validation paths are shown in Figures 9 and 10 on an arbitrary global reference frame.

These figures show the real paths as computed by means of the successive laser scan localization method. Walls and other environment objects perceived by the sensor are shown as clouds of points around the path. In addition, these figures show estimations of the paths based on odometry alone (i.e., drive shaft encoders) according to the approximate kinematic models identified in Section 5.

Similar conclusions can be drawn from both validation paths. The less accurate dead reckoning estimation corresponds to the simple experimental symmetric model. Interestingly, the asymmetric ICR model obtained by simulation does not improve much this result. This can be explained by simplifications and imprecisions introduced in the dynamic model, as well as by the fact that the track ICRs have been obtained as the average of the whole ICR map, regardless of the combinations occurring in actual paths. This way, the experimental asymmetric model achieves a significant improvement in dead reckoning performance.

Moreover, the training experiments described in Section 5 have also been used to perform a GA search for fine-tuning parameters α_l and α_r in eqs. (20) and (21). After introducing the resulting corrections (α_l = 1.0072 and α_r = 1.0275) in all three kinematic models evaluated above, the dead reckoning estimations provide the paths shown in Figures 11 and 12. All the solutions are now closer to the original path, while the relative accuracy between the three models remains intact. The GA-based experimental kinematic model achieves impressive results that are very similar to dead reckoning for well-calibrated wheeled robots.

Note that results in path 2 are better than in path 1, since it is softer in curvature and speed variations. This conclusion is also usual in dead reckoning for wheeled vehicles. Once constant model parameters have been obtained, dynamics is no longer considered, so the model is subject to dynamics-related non systematic errors in odometry (Borenstein and Feng 1996).

7. Conclusions

The work presented in this paper originates from the need to control the motion of a tracked autonomous mobile robot. The aim was to improve real-time navigation by considering the effects of track slippage, but without introducing the complexity of dynamics computations in the loop. An approximate kinematic model is an effective solution to this problem.

We have established a common differential drive kinematic model for both tracked and wheeled traction, based on the ICRs of the treads on the plane with respect to the vehicle. It has been shown that slippage affects the positions of tread ICRs during navigation. Thus, in the case of ideal drive wheels, ICRs lie constantly on the ground contact points; for a track, this position varies within a bounded area some distance away from the tread centerline.

An approximate kinematic model for tracked vehicles results from estimating constant positions for its track ICRs. This model represents an equivalent ideal differential drive wheeled vehicle, so conventional path tracking methods

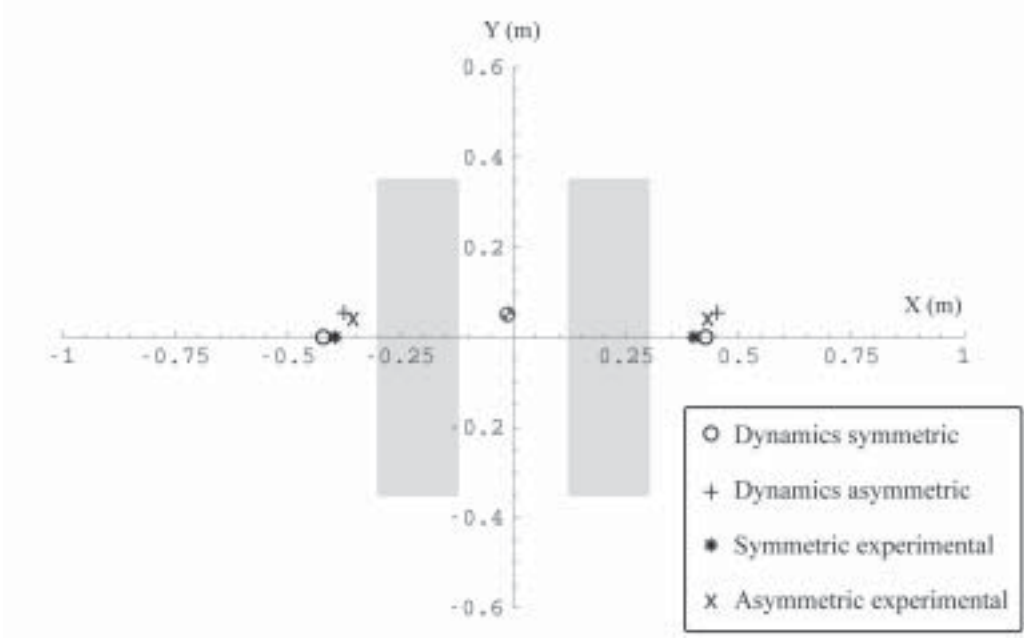

Fig. 8. Summary of track ICR estimations.

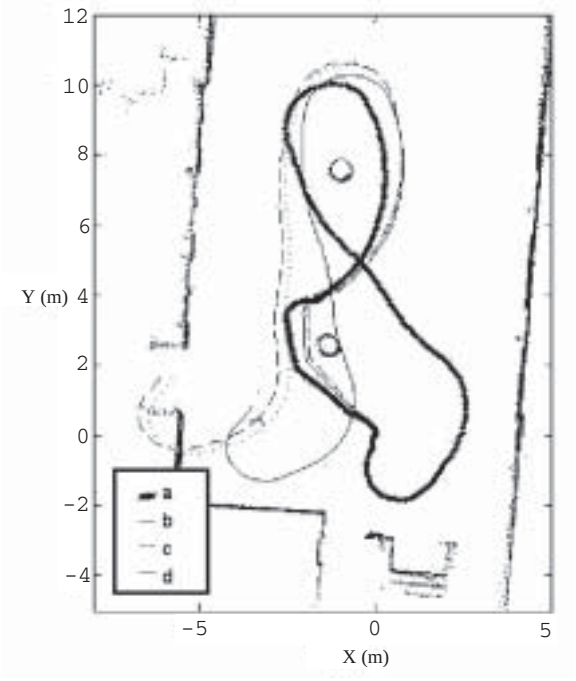

Fig. 9. Validation path 1: (a) real path; (b) asymmetric ICRs from dynamic simulation; (c) experimental symmetric ICRs; (d) asymmetric ICRs from GA identification.

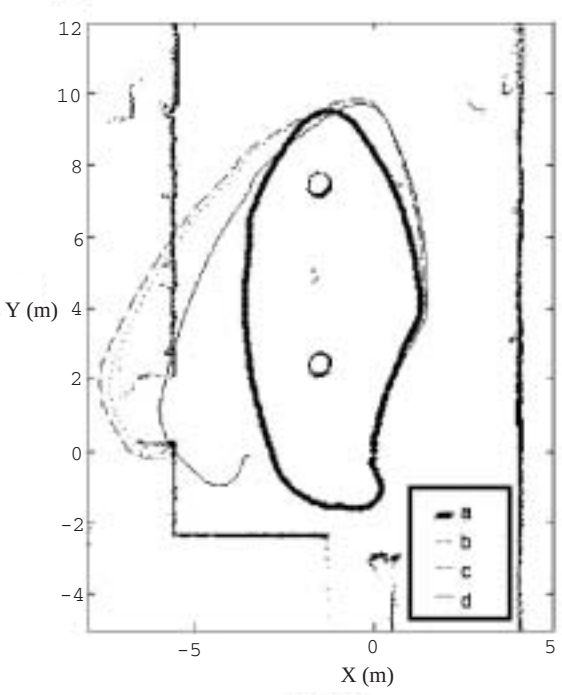

Fig. 10. Validation path 2: (a) real path; (b) asymmetric ICRs from dynamic simulation; (c) experimental symmetric ICRs; (d) asymmetric ICRs from GA identification.

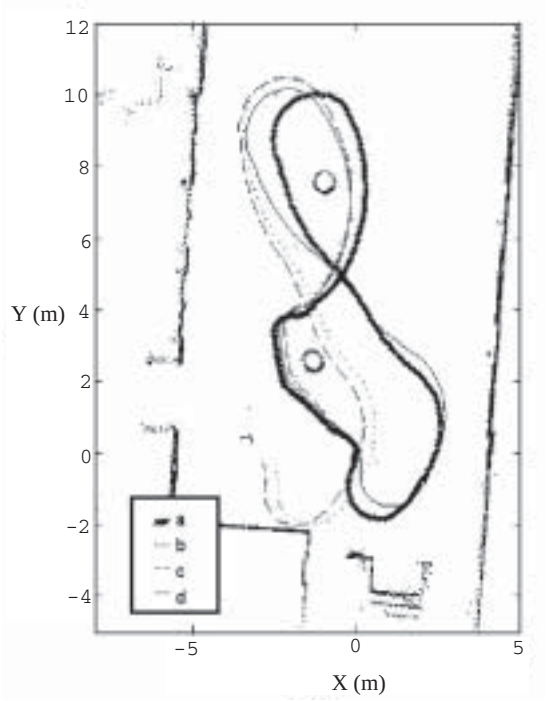

Fig. 11. Validation path 1 with additional fine-tune search parameters: (a) real path; (b) asymmetric ICRs from dynamic simulation; (c) experimental symmetric ICRs; (d) asymmetric ICRs from GA identification.

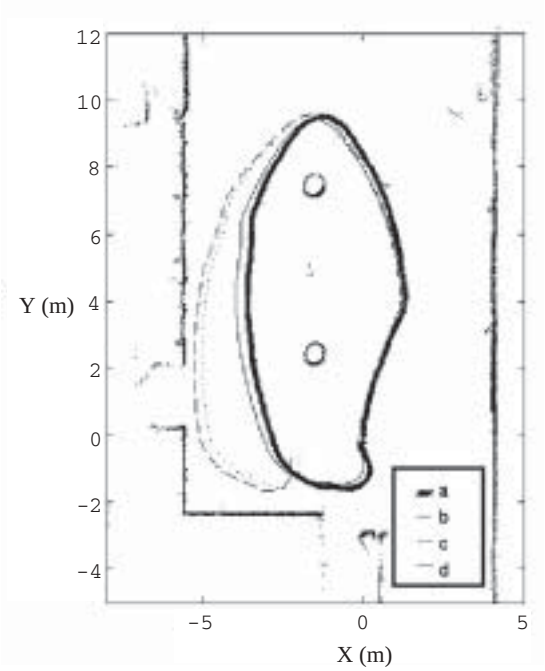

Fig. 12. Validation path 2 with additional fine-tune search parameters: (a) real path; (b) asymmetric ICRs from dynamic simulation; (c) experimental symmetric ICRs; (d) asymmetric ICRs from GA identification.

can be employed effectively without modifications. Several approaches have been proposed in order to obtain this approximation.

The simulation of a dynamic model of the vehicle with track–soil interactions allows computing a map of track ICR positions for the whole working range of combined track speeds. This way, a constant position for each track can be estimated so that it best fits the map.

Besides, two experimental methods have been proposed. First, a simple experiment produces a rough estimation of the apparent positions of symmetrical ideal wheels. Secondly, optimization techniques can be used to search for constant ICRs given a specific robotic task, according to typical path motions, particular soil types, and speed ranges. In this case, a GA is proposed that uses sensor data from representative real paths.

Coherent results have been obtained from the application of all the proposed methods to the Auriga-α tracked mobile robot on a hard-surface flat soil. For instance, both the simulation of the dynamic model and the GA search have detected asymmetries in ICR positions due to the center of mass of the vehicle. Furthermore, GA search allows for experimentally fine-tuning nominal vehicle parameters, such as the ratio between drive shaft velocity and track speed. From the implementation standpoint, the development of the dynamic model has been costly and its results are affected inevitably by design simplifications, but it allows qualitative evaluation. On the other hand, the GA approach requires reliable pose estimations along the path, but parameter sets can easily be obtained from a number of different terrains.

Performance of the approximate model has been evaluated by running a number of validation paths with Auriga-α. The motion control accuracy (i.e., pose estimation given a history of odometric readings, and computation of control inputs so that the robot can obtain desired motion) has been clearly improved with respect to our previous solutions. Odometric estimations have been particularly accurate for the GA approximation.

Even if results have been favorable for a scenario that represents many autonomous robot applications, it would be interesting to test the proposed approach with other types of terrains and different tracked vehicles. Moreover, the method could even be applied to introduce dynamic-based adjustments to kinematic models of non-ideal differential drive wheeled robots, since these are always affected by some degree of slippage. This is especially true for wheels with large contact areas, such as poorly inflated pneumatic tires or wheeled skid-steered vehicles.

Acknowledgments

This work was partially supported by the Spanish project DPI 2002-04401-C03-01.

References

Ahmadi, M., Polotski, V., and Hurteau, R. 2000. Path tracking control of tracked vehicles. *Proceedings of the IEEE International Conference on Robotics and Automation*, San Francisco, CA, pp. 2938–2943.

Bekker, M. G. 1956. *Theory of Land Locomotion*, University of Michigan Press, Ann Arbor, MI.

Borenstein, J. and Feng, L. 1996. Measurement and correction of systematic odometry errors in mobile robots. *IEEE Transactions on Robotics and Automation* 12(6):869–880.

Fan, Z., Koren, Y., and Wehe, D. 1995. Tracked mobile robot control: hybrid approach. *Control Engineering Practice* 3(3):329–336.

Fan, Z., Borenstein, J., Wehe, D., and Koren, Y. 1995. Experimental evaluation of an encoder trailer for dead-reckoning in tracked mobile robots. *Proceedings of the IEEE International Symposium on Intelligent Control*, Monterey, CA, pp. 571–576.

Ferretti, G. and Girelli, R. 1999. Modeling and simulation of an agricultural tracked vehicle. *Journal of Terramechanics* 36:139–158.

Kar, M. K. 1987. Prediction of track forces in skid-steering of military tracked vehicles. *Journal of Terramechanics* 24(1):75–86.

Le, A. T., Rye, D. C., and Durrant-Whyte, H. F. 1997. Estimation of track–soil interactions for autonomous tracked vehicles. *Proceedings of the IEEE International Conference on Robotics and Automation*, Albuquerque, NM, Vol. 2, pp. 1388–1393.

Mandow, A., Gómez-de-Gabriel, J. M., Martínez, J. L., Muñoz, V. F., Ollero, A., and García-Cerezo, A. 1996. The autonomous mobile robot Aurora for greenhouse operation. *IEEE Robotics and Automation Magazine* 3(4):18–28.

Martínez, J. L. 2003. Mobile robot self-localization by matching successive laser scans via genetic algorithms. *Proceedings of the 5th IFAC International Symposium on Intelligent Components and Instruments for Control Applications*, Aveiro, Portugal.

Martínez, J. L., Mandow, A., Morales, J., García-Cerezo, A., and Pedraza, S. 2004. Kinematic modeling of tracked vehicles by experimental identification. *Proceedings of the IEEE/RSJ International Conference on Intelligent Robots and Systems*, Sendai, Japan, pp. 1487–1492.

Ollero, A., García-Cerezo, A., Martínez, J. L., and Mandow, A. 1997. Fuzzy tracking methods for mobile robots. *Applications of Fuzzy Logic: Towards High Machine Intelligence Quotient Systems*, Series on Environmental and Intelligent Manufacturing Systems, Prentice-Hall, Englewood Cliffs, NJ, Vol. 9, Chap. 17, pp. 347–364.

Pedraza, S. 2000. Modeling and analysis of tracked vehicles for autonomous navigation, Ph.D. Thesis, University of Málaga, Spain (in Spanish).

Pedraza, S., Fernández, R., Muñoz, V. F., and García-Cerezo, A. 2000. A motion control approach for a tracked mobile robot. *Proceedings of the 4th IFAC International Symposium on Intelligent Components and Instruments for Control Applications*, Buenos Aires, Argentina , pp. 147–152.

Shigley, J. E. and Uicker, J. J. 1980. *Theory of Machines and Mechanisms*, McGraw Hill, New York.

Shiller, Z., Serate, W., and Hua, M. 1993. Trajectory planning of tracked vehicles. *Proceedings of the IEEE International Conference on Robotics and Automation*, Atlanta, GA, Vol. 3, pp. 796–801.

Wang, G. G., Wang, S. H., and Chen, C. W. 1990. Design of turning control for a tracked vehicle. *IEEE Control Systems Magazine* 10(3):122–125.

Wong, J. Y. 2001. *Theory of Ground Vehicles*, 3rd edition, Wiley, New York.